A Framework for the Generation of Realistic Brain Tumor Phantoms and Applications

Jan Rexilius[1], Horst K. Hahn[1], Mathias Schlüter[1], Sven Kohle[1], Holger Bourquain[1], Joachim Böttcher[2], and Heinz-Otto Peitgen[1]

[1] MeVis – Center for Medical Diagnostic Systems and Visualization, Bremen, Germany
rexilius@mevis.de
[2] Department of Diagnostic and Interventional Radiology, University of Jena, Germany

Abstract. A quantitative analysis of brain tumors is an important factor that can have direct impact on a patient's prognosis and treatment. In order to achieve clinical relevance, reproducibility and especially accuracy of a proposed method have to be tested. We propose a framework for the generation of realistic digital phantoms of brain tumors of known volumes and their incorporation into an MR dataset of a healthy volunteer. Deformations that occur due to tumor growth inside the brain are simulated by means of a biomechanical model. Furthermore, a model for the amount of edema at each voxel is included as well as a simulation of contrast enhancement, which provides us with an additional characterization of the tumor. A "ground truth" is generally not available for brain tumors. Our proposed framework provides a flexible tool to generate representative datasets with known ground truth, which is essential for the validation and comparison of current and new quantitative approaches. Experiments are carried out using a semi-automated volumetry approach for a set of generated tumor datasets.

1 Introduction

Magnetic resonance imaging (MRI) has become an important imaging modality for diagnosis and treatment planning of brain tumors. The main forms of treatment are surgery, radiation therapy, and chemotherapy [1]. A fundamental issue is the accuracy of the calculated quantitative parameters which can have direct impact on therapy. The tumor volume is often used as an objective parameter. However, since brain tumors can largely vary in size, shape, amount of edema, and enhancement characteristics, any quantification of the tumor volume used in clinical routine and in multi-center studies has to be carefully evaluated. Varying acquisition protocols and image quality add to complexity of this task.

Several computer assisted methods have been proposed for the segmentation and quantification of brain tumors [2,3,4,5]. However, due to the absence of a "ground truth" for brain tumors, computation of the exact volume is still a challenging problem. A common approach for the validation of quantitative image analysis methods of brain tumors is based on manual segmentation performed by a medical expert. Since this approach is inherently subjective to interobserver variations and human error, analyses of several experts for the same tumor are usually considered in combination [2].

C. Barillot, D.R. Haynor, and P. Hellier (Eds.): MICCAI 2004, LNCS 3217, pp. 243–250, 2004.

Established and representative datasets with known ground truth are essential for the validation and comparison of current and new approaches. A flexible way to generate realistic phantom datasets with exactly known ground truth could be a step towards this goal. Available physical phantoms typically consist of simple objects that are placed in an MR scanner [6]. Digital phantoms can cover a broader range of distributions of shape, size, and contrast behavior. A ditigal phantom for the brain is available from the BrainWeb project [7]. A phantom for Multiple Sclerosis lesions was proposed in [8]. However, there are no suitable phantoms available for brain tumors.

The aim of this paper is to introduce a new approach for the validation of quantitative analyses of brain tumors. We propose a framework for the generation of realistic tumor phantoms of known volumes incorporated in an MRI scan. Brain tumors have a high variabilitly in appearance, size, location, and structure. We focus on glial tumors (gliomas), that constitute the most common group of primary intracranial neoplasms [1]. The biomechanical model used in this paper allows us to simulate deformations that occur due to tumor growth inside the brain. An experimental study is carried out using a semi-automated volumetry approach for a set of generated tumor datasets. In addition, we provide a simulation of contrast agent enhancement characteristics for the tumor phantom.

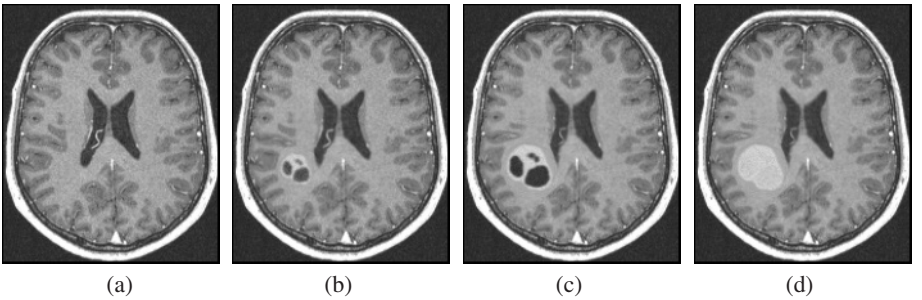

(a) (b) (c) (d)

Fig. 1. Examples of tumor phantoms without simulation of edema that differ only in size and amount of necrosis in comparison to original MR data. (a) Original T1-weighted image post contrast (T1gd) of healthy volunteer; (b) T1gd image with small tumor; (c) T1gd image with large tumor; (d) T1gd image with large tumor and necrotic tissue scaled to 5%.

2 Modeling Active Tumor Tissue and Necrosis

An issue of specific clinical relevance for a quantitative analysis of brain tumors is the proof of validity of a proposed method. Because of the lack of a “ground truth" for comparison we develop a framework for the generation of datasets with realistic brain tumor phantoms. Essential requirements for the development of our phantoms are (a) a known volume of each tumor to test the accuracy of an investigated method, (b) the possibility to fexibly generate tumors in terms of shapes, sizes, etc., and (c) plausibility with respect to clinical image data. Due to its complex microscopic structure, the tumor

phantoms proposed in this work are simulated on a macroscopic level consisting of merely two tissue classes, namely active tumor tissue and necrosis (cf. Figs. 1, 2).

The generation of a phantom dataset consists of two basic steps. In a first step, a high-resolution and arbitrarily shaped tumor phantom with known volume is defined. Then, it is incorporated into an MR scan of the brain of a normal volunteer. A similar concept was used in [8] to generate realistic phantoms of small white matter lesions that occur in patients with Multiple Sclerosis.

2.1 Generation of Brain Tumor Phantoms

Approximation of a continuous volume model. We generate high-resolution binary phantom volumes $i_p : \Theta \rightarrow \{0, 1\}$ with signal intensity values $i_p(\mathbf{x}) \in \{0, 1\}$ at voxel positions $\mathbf{x} = (x, y, z)^\top$, $\mathbf{x} \in \Theta$ for the two available tissue classes. A small voxel size is used in order to provide an appropriate approximation of the continuous object volume $V_{i_p} = \int_\Theta i_p(\mathbf{x}) d\mathbf{x}$. Different volumes can be easily generated by specifying a different voxel size. To ensure the validity of this assumption, the voxel size for the largest phantom volume is set more than five times smaller than that of the available MR images. In this work we choose tumor volumes between 2 ml and 20 ml.

Both, active tumor tissue and necrosis are drawn non-overlapping on a 256^3 grid with a number of voxels set to gray value 1, so that the underlying ground truth can be extracted for both classes separately. For the figures presented in this work, a shape based on a manual segmentation of a patient dataset with a real brain tumor is used.

Accounting for partial volume effects. In order to incorporate the two previously generated phantom volumes into an MR scan of the brain ($i_b : \Omega \rightarrow \mathbb{R}$ with intensity values $i_b(\mathbf{x})$), they are downsampled to the same voxel size as the MR scan, using trilinear interpolation and then reformatted into the coordinate system of the MR scan. This results in a probability map $\tilde{i_p} : \Omega \rightarrow \in [0, 1]$ with intensity values $\lambda := \tilde{i_p}(\mathbf{x})$ for each modeled tissue class. Various stages of necrosis can be modeled by scaling each voxel of the original binary image between 0 and 1 (Figure 1 d).

Generation of tumor gray values. We generate volumes i_t for active tumor and necrosis containing reasonable gray values for each available sequence. Furthermore, Gaussian noise is added approximately set equal to the noise of the brain scans. In order to account for a more complex appearance, different noise models could be applied, e.g., based on a Gibbs sampler.

To summarize, this method provides us with a flexible set of rules to generate a realistic tumor phantom with known ground truth that can be incorporated into a dataset of the brain. Tumor phantoms for other organs could be simulated as well using this approach.

2.2 Biomechanical Modeling of Deformations Induced by Tumor Growth

An important aspect in generating a realistic phantom for brain tumors is to simulate the deformation imposed by the tumor growth. A fundamental assumption thereby is

that surrounding brain tissue is pushed away from the tumor. In order to gain insight into the process of tumor growth, mathematical modeling has become an increasingly important role and various methods have been proposed. See [9] and references therein. Especially cellular automaton models, that describe the spread and invasion of a tumor on a cell interaction level, have become a popular tool. An approach that simulates the tumor growth on a rather macroscopic level using continuum mechanics was proposed in [10].

In this work, we simulate the three-dimensional tumor growth based on a linear elastic model, which was previously also used to capture shape changes of the brain during neurosurgery [11,12]. Since a rigid model can be assumed for surrounding tissue such as the dura mater, the model is constrained at the boundaries of a brain mask generated by a modified watershed transform [13], so that motion is restricted to areas inside the brain. In order to simulate tumor growth, we place our phantom at an arbitrary position inside the brain with a given radial displacement $u(\mathbf{d}) = \alpha\mathbf{d}, \alpha \in \mathbb{R}^+$ in each direction $\mathbf{d} \in \mathbb{R}^3$. The center of gravity of the tumor phantom is used as point of origin. The computed constraints for both, tumor and brain boundary are then introduced as external forces into the elastic model. Thus, changes in the shape of the brain are modeled to result in an equilibrium state of energy with a displacement u that minimizes the total potential energy given as

$$E(u) = \frac{1}{2} \int_{\Omega} \sigma^{\top} \epsilon \, d\Omega \; - \; \int_{\Omega} F^{\top} u \, d\Omega \; . \tag{1}$$

The variables are given in terms of the strain vector, σ, the stress vector, ϵ, and the external forces, F [14]. Assuming homogeneous, isotropic material, the mechanical behavior of brain tissue undergoing deformation is described by Young's modulus E ($E = 3kPa$) and Poisson's ratio ν ($\nu = 0.4$). The resulting equation is solved by a finite element approach [14]. A fast parallel implementation was proposed in [12] as part of a nonrigid registration approach.

In order to also simulate the process of tumor growth, we initially start with a deformation restricted to the boundary of a downsampled (factor 5) phantom, with its center of gravity placed at the same position as for the full-scale tumor phantom. Thus, even brain structures very close to or even inside the full-scale phantom's boundaries can be pushed away from the tumor. In a further step, we track the deformation for each voxel by iterating on the deformation field

$$u_n(\mathbf{x}) = u_{n-1}(\mathbf{x}) + u(\mathbf{x} + u_{n-1}(\mathbf{x})) \; . \tag{2}$$

The maximum deformation in the full-scale phantom size is set as stopping criterion for the iteration process. The amount of displacement per iteration varies with the scale factor α as defined above.

It should be noted that although more accurate modeling of tumor growth would be desirable, e.g. [15], it is not essential for the proposed aim of a model for quantitative image analysis.

2.3 Incorporation of a Tumor Phantom into an MR Scan

In a final step, the tumor phantom is incorporated into an MR dataset. Three-dimensional T1-weighted pre and post contrast as well as T2-weighted MR data from a healthy

volunteer were used as basis in this work (Siemens Magnetom Vision 1.5T, 256x256 matrix, 1.0mm isotropic voxel size).

In order to simulate the deformation induced by tumor growth as described in the previous section, the generated displacement field is applied to warp the MR data. The resulting phantom dataset is then generated as a linear combination of the deformed MR scan $\tilde{i_b}$ and the tumor volumes $\tilde{i_t}$, containing appropriate gray values for the modeled tumor tissues, i.e. active tumor and necrosis. Thus, new signal intensity values are defined as the convex combination

$$\tilde{i_b} \;=\; \sum_{j=1}^{N}\big(\lambda_j \cdot \tilde{i_{j,t}}\big) \;+\; \big(1-\sum_{j=1}^{N}\lambda_j\big)\cdot \tilde{i_b}, \qquad \lambda_j \in [0,1], \tag{3}$$

where N ist the number of modeled tumor tissue classes (here $N = 2$), and the resulting value is assigned to each voxel of the MR dataset. Figures 1 and 2 illustrate some results.

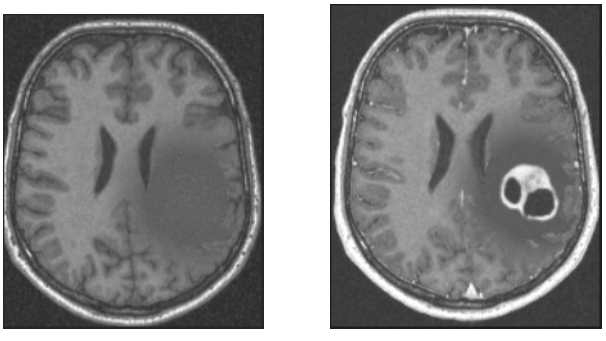

Fig. 2. Tumor phantom along with a simulation of edema introduced on a T1-weighted image pre and post contrast.

3 Modeling Edema

In addition to the actual tumor, edema is another important structure that should be taken into account for a realistic model of brain tumor phantoms. Brain edema is an inflammatory response to the tumor, which causes, the brain around the tumor to swell and is mostly located in the white matter [1]. Since the brain is located in a confined space and cannot expand, and because the fluid that accumulates cannot easily be carried away, an edema can impair the normal functioning of the brain and causes an increase of intracranial pressure. Therefore, accurate segmentation and quantitative analyses could add valuable information for a physician. Recently, a method for tumor segmentation with an explicit model for edema was proposed in [5].

In order to generate a model for edema we simulate the amount of edema at each voxel, and thus the amount of partial volume, using a geodesic distance transformation [16] starting from the tumor. The basic idea is to constrain the distance computation

to remain within a subset of the image volume. As for the edema, we use a white matter mask, since the edema is usually located in the white matter of the brain. To account for tumor growth, we apply the same deformation field as for the MR data before calculating the distance. Depending on the resulting distance map we define a region of pure edema and mixture between pure edema and normal brain tissue, i.e., various degrees of edema dissemination can be simulated this way. The amount of partial volume is scaled accordingly. Further partial volume effects that occur between edema and tumor tissue at the boundary of the tumor are considered as well. A suitable gray value and noise level are defined similar to the method decribed in Section 2.1. In order to finally incorporate edema into the MR scan, Equation 3 is extended by a new tissue class, i.e., $N = 3$.

4 Experimental Results

To evaluate the framework for brain tumor phantoms presented in this paper, we show results for two different applications, namely a semi-automated volumetry method with explicit partial volume modeling and a simulation of contrast enhancement characteristics based on a two-compartment model. All algorithms have been integrated into the research and development platform Me*VisLab* [17].

4.1 Robust Semi-automated Volumetry

We evaluated 3 phantom MR datasets generated from a brain scan of a normal volunteer. The proposed semi-automated volumetry method combines a 3d marker based segmentation and a multimodal histogram analysis with an explicit model for partial volume effects. In a first step, a fast skull stripping algorithm based on a modified watershed transform is applied to generate an coarse segmentation [13]. Then, the model parameters used for classification are adapted with a maximum likelihood mixture model clustering algorithm on the T1- and T2-weighted images similar to that proposed in [18]. Table 3 compares the semi-automated volumetry method with the known ground truth for each phantom. Our results show an overestimation between 0.15% and 7%.

	Ground Truth	Semi-Automatic
Tumor 1	2.0 ml	2.14 ml
Tumor 2	10.0 ml	10.07 ml
Tumor 3	20.0 ml	20.03 ml

Fig. 3. Results of semi-automatic partial volume analysis for three different brain tumor phantoms with known ground truth.

4.2 Simulation of Contrast Enhancement Characteristics

Multi-compartment models are commonly used to describe the enhancement of macromolecular contrast agent particles in tumor tissue and thus are an important tool for

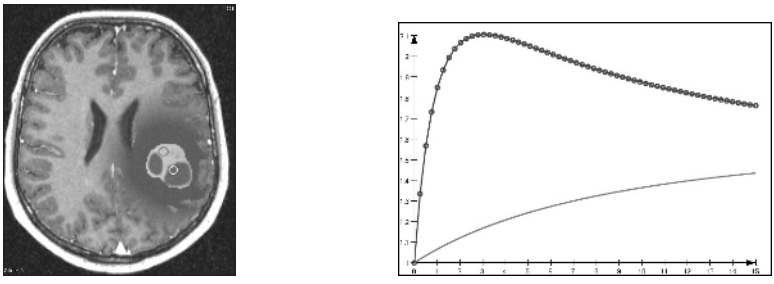

(a) (b)

Fig. 4. Results of simulated enhancement characteristics for a T1-weighted gradient echo sequence. The imaging parameters were adapted to the parameters of the real MR scan (TE=5ms, TR=15ms, FlipAngle=30°). (a) Enhancement of tumor tissue. the region drawn in the tumor correspond to the curves in the diagram; (c) enhancement curves for selected regions inside the tumor (horizontal: time in minutes, vertical: relative enhancement). For active tumor tissue the simulation results in a rapidly increasing curve due to high values in the generated permeability parameter map.

computer assisted analysis of dynamic MRI. We have implemented the Tofts&Kermode model [19] in order to generate simulated perfusion datasets. This enables us to combine the prediction of contrast agent enhancement and a known ground truth for a quantitative analyis in simulated brain tumors. In order to apply the Tofts&Kermode model to the tumor phantom, we generate maps for the artificial distribution of physiologic parameters: the permeability of tissue and the extracellular volume fraction which is accessible for the contrast agent. For the permeability we assume an increase from the center to the border of the tumor, where most of the active tumor tissue is usually located. Therefore, an euclidean distance transform is used. A very low permeability is assigned to necrotic tissue using the simulated amount at each voxel as a scaling factor. The extracellular volume fraction is assumed to vary only slightly between $0.7 - 0.8$. Here, we set a higher value for necrosis than for active tumor tissue. Figure 4 exemplary shows the resulting gray values one time-point as well as the enhancement curves for different positions inside the tumor. We generated a simulation of contrast enhancement at a 0.5 minutes scan-interval up to 15 minutes after injection of contrast agent at a dose of 0.1mmol/kg.

5 Discussion and Conclusion

Our main objective in this work has been to develop and test a framework for the generation of realistic phantoms for brain tumors with exactly known volumes for active tumor, necrosis, and edema. Therefore, an arbitrarily shaped high-resolution phantom is incorporated into an MR scan of a normal volunteer. A biomechanical model enables us to simulate deformations that occur due to tumor growth inside the brain. Furthermore, important additional properties such as the amount of edema at each voxel as well as a simulation of contrast enhancement can be provided for the tumor phantom.

Future work will investigate the accuracy and reproducibility of different volumetry methods. Therefore, our proposed framework can provide a realistic basis for validation. New methods that account for preferred tumor dissemination pathways will provide a more accurate basis for the tumor and edema growth, e.g., maps of the principal diffusivity directions derived from diffusion tensor imaging. In order to provide a new tool for comparison in tumor volumetry, our approach could be used to generate a database with a set of brain tumor phantoms.

References

1. A.G. Osborn, K.A. Tong. Handbook of Neuroradiology: Brain and Skull, 2nd edition. Mosby-Year Book, Inc, Missouri, 1991.
2. M. Kaus, S.K. Warfield, A. Nabavi, et al. Automated Segmentation of MR Images of Brain Tumors *Radiology*, 218(2):586-91, 2001.
3. G. Moonis, J. Liu, J.K. Udupa, D.B. Hackney. Estimation of Tumor Volume with Fuzzy-Connectedness Segmentation of MR Images *Am J Neuroradiol*, 23(3):356-63, 2002.
4. J.-P. Guyon, M. Foskey, J. Kim, et al. VETOT, Volume Estimation and Tracking Over Time: Framework and Validation. *MICCAI 2003* vol 2879 of LNCS, pp. 142-149, 2003
5. M. Prastawa, E. Bullitt, N. Moon, et al. Automatic Brain Tumor Segmentation by Subject Specific Modification of Atlas Priors. *Acad Radiol*, 10:1341-1348, 2003.
6. P.S. Tofts, G.J. Barker, M. Filippi, M. Gawne-Cain, M. Lai. An oblique cylinder contrast-adjusted (OCCA) phantom to measure the accuracy of MRI brain lesion volume estimation schemes in multiple sclerosis. *J. Magn Reson Imaging*, 15(2):183-192, 1997.
7. D. Collins, A. Zijdenbos, V. Kollokian, et al. Design and Construction of a Realistic Digital Brain Phantom. *IEEE TMI*, vol. 17, no. 5, pp. 463-468, 1998.
8. J. Rexilius, H.K Hahn, H. Bourquain, H.-O. Peitgen. Ground Truth in MS Lesion Volumetry – A Phantom Study. *MICCAI 2003*, vol 2879 of LNCS, pp. 546-553, 2003.
9. A.R. Kansal, S. Torquato, G.R. Harsh et al. Simulated Brain Tumor Growth Dynamics Using a Three-Dimensional Cellular Automaton, *J Theor Biol.* 203(4): 367-382, 2000.
10. R. Wasserman, R. Acharya, C. Sibata, K.H. Shin. A Patient-Specific In Vivo Tumor Model. *Math Biosci.*, 136(2):111-40, 1996.
11. M. Ferrant, A. Nabavi, B. Macq, et al. Registration of 3D interoperative MR images of the brain using a finite element biomechanical model *IEEE TMI*, vol. 20(12):1384-1397, 2001.
12. J. Rexilius, S.K. Warfield, C.R.G. Guttmann, et al. A Novel Nonrigid Registration Algorithm and Applications. *MICCAI 2001*, pp. 923-931, 2001.
13. H.K. Hahn, H.-O. Peitgen. The Skull Stripping Problem in MRI Solved by a Single 3D Watershed Transform *MICCAI 2000*, pp. 134-143, 2000.
14. O.C. Zienkewickz, R.L. Taylor. The Finite Element Method. McGraw Hill Book Co., 1987.
15. J. Modersitzki. Numerical Methods for Image Registration. Oxford University Press, 2004.
16. P. Soille. Morphological Image Analysis: Principles and Applications, 2nd edition. Springer-Verlag Berlin, 2003.
17. Me*VisLab* 1.0, (c) 2004 MeVis gGmbH. Available at: http://www.mevislab.de.
18. A. Noe, J.C. Gee. Partial Volume Segmentation of Cerebral MRI Scans with Mixture Model Clustering. *IPMI 2001*, 423-430, 2001.
19. P.S. Tofts, A.G. Kermode. Measurement of the Blood-Brain Barrier Permeability and Leakage Space Using Dynamic MR Imaging. 1. Fundamental Concepts. *Magn Reson Med*, 17:357-367, 1991.